COMSOL
CONFERENCE
2024 FLORENCE

3D Thermal Analysis of Complex Cable Crossings

P. Zairis, D. Chatzipetros, T. Liangou, K. Bitsi, A. I. Chrysochos
Hellenic Cables, Athens, Greece.

Abstract
The proximity of heat sources, such as steam pipes or other loaded cables, to cables under installation may significantly affect their thermal performance. When the adjacent heat sources are installed in parallel, 2D analysis is sufficient to represent the heat transfer problem. However, when these heat sources cross each other under some crossing angle, the longitudinal heat cooling along the cable metallic components, such as cable conductor, may significantly improve the cable current rating. Further to the existing literature that assumes the cables under crossing are totally straight, this paper deals with cable installations, such as those in High Voltage substations, where the cables are bent before reaching the crossing points. 3D analysis is inevitable in such complex installation cases. A Finite Element Method model is developed in the present paper. By taking advantage of the high computational resources, geometric tips and proper solver settings, the crossing model becomes feasible to launch at reasonable execution times. Results are compared against those derived from published methods in the existing literature.

Keywords: Cable crossings, FEM, modelling, optimization, underground cables.

Introduction
By restructuring the electricity industry and introducing the electricity market around the world, the transmission lines have been becoming increasingly loaded. Apart from the operating voltage, the transmission performance of an underground cable line is determined by its current carrying capacity (ampacity) that is limited by the most unfavorable thermal conditions along the entire cable line route.
The simplest way of incorporating the mutual effect of neighboring cables to the cable under consideration is via the modification in the cable external resistance, T_4. This can be very easily done when cables are laid in parallel, as suggested by the IEC 60287-2-1 Standard analytical method [1] for various cable configurations. However, this method becomes overly conservative when considering cable crossings.
A method considering the longitudinal heat flux in the cable based on analytical formulae has been proposed in [2], [3]. To make the formulation even simpler, the heat flux is assumed to propagate exclusively along the conductor. Cycling loading included in [4], soil drying-out in [4], [5], and heat transfer along the metallic sheath in [5], [6] are other improvements being proposed in the existing literature. The IEC 60287-3-3 Standard method [7] describes an analytical, accurate method to calculate the continuous current rating factor for cables crossing with other external heat sources. This method relies on the previous algorithms and the principle of superposition, being applicable to any cable type. The maximum permissible current is obtained by multiplying the continuous rating of the cable as though this was isolated by a derating factor related to a mutual thermal resistance between cable and crossing heat source. In the case of studying multiple heat sources crossing the cable, the IEC Standard method can be, theoretically, generalized when the hottest point is defined. This, however, has been proved to be a cumbersome task, demanding repetitive calculations at several points to ensure the hottest point is found. An analytical method capable of calculating the cable ampacity where multiple cables cross each other under various crossing angles has been recently presented in [8] by some of the authors. However, in this method the cables are assumed to be absolutely straight before reaching the crossing point, thus being questionable for cables under bend, which is a more realistic condition within High Voltage (HV) substations.
In this work, the thermal behaviour of more than 20 cable crossings consisting of cables of different voltage levels, from Low Voltage (LV) cables to Extra High Voltage (EHV) cables, installed in various depths and angles, is analyzed. This is an actual installation case used at a real HV substation. To the best of the authors' knowledge, this is the first time in the existing literature that such a complicated geometry, including bent cables in multiple crossing points, is examined. The results derived from the proposed method are evaluated against those from analytical methods existing in the present literature. The findings of this work are useful for the optimization of cable design under special installation conditions, such as those inside HV substations.

Problem definition
The current carrying capacity of a cable, often called 'ampacity', is limited by the thermal environment

along its entire route. Hot spots may occur when underground cables cross various heat sources, mainly other power cables and heating pipelines. These hot spots represent the areas where the cable temperature may exceed the design limit of the cable main insulation, i.e., 90 °C for XLPE.
In the installation case studied in the present work (Figure 1), cables are installed under different installation conditions (directly buried, inside plastic ducts or in concrete troughs), either in trefoil formation (Figure 2) or in flat formation (Figure 3). Circulating and eddy current losses are applied according to IEC 60287-1-1 [9], assuming magnetically isolated cable circuits for simplicity.

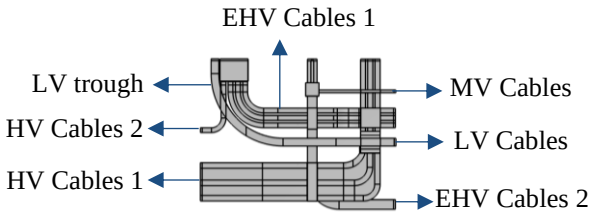

Figure 1. Underground cable installation inside HV substation – Top view

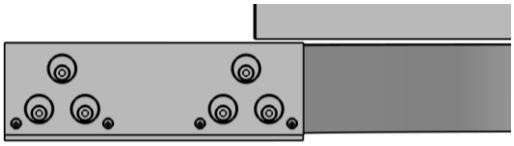

Figure 2. Cables installed in trefoil formation – Side view.

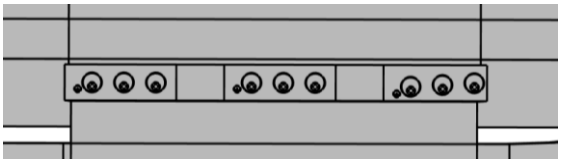

Figure 3. Cables installed in flat formation – Side view.

Different types of cables and surrounding medium are used in this specific case study. The materials used for the analysis are shown in Table 1.

Table 1. Properties of cables and surrounding medium.

Layer	Variable	Value
Copper/Aluminum conductor	ρ_t [Km/W]	0.0026 / 0.0049
Conductor tape		12
Conductor screen layer		2.5
PVC/XLPE insulation		6 / 3.5
Insulation screen layer		2.5
Copper wire screen		0.0026
Aluminum sheath		0.0049
PVC/HDPE jacket		6 / 3.5
Outer semiconductive layer		2.5
Surrounding medium		
Sand	ρ_t [Km/W]	1.23
Fine sand		0.8
Concrete		0.6

Governing Equations and Simulation Methods

Applied physics and modelling approach

To account for the thermal effect of the crossings, this analysis can only be conducted in three dimensions. Heat transfer in Solids and Surface-to-Surface Radiation physics are solved with the appropriate boundary conditions applied. Natural convection is also considered, using analytical equations, as described below.
Infinite domains (Figure 4) are also introduced on the sides to represent the semi-infinite space and extend the solution mathematically towards infinity, where thermal insulation boundary condition is applied. [10], [11]
Considering the installation conditions, part of the MV and EHV cables and the LV cables are installed within troughs (Figure 4). The troughs are made by concrete and are in contact with the external environment. Hence, surface to ambient radiation is applied to their top surfaces, as shown in Figure 5. The ambient temperature of the troughs is considered equal to 55ºC, 40ºC (ambient temperature on trough surface) plus 15ºC, to account for the effect of solar radiation, according to [10]. Surface to Ambient radiation is also applied to the soil surface considering an ambient temperature of 25ºC. The consideration of different ambient temperature values for the troughs and the soil does not have any physical meaning. It is related to the way the current rating of the cables is determined. In the case of cable installed within troughs, the cable ambient temperature is likely to be affected more directly by solar radiation leading to higher ambient temperature compared to that of deep installations, hence, it is not also correct to rate these cables in the same way.

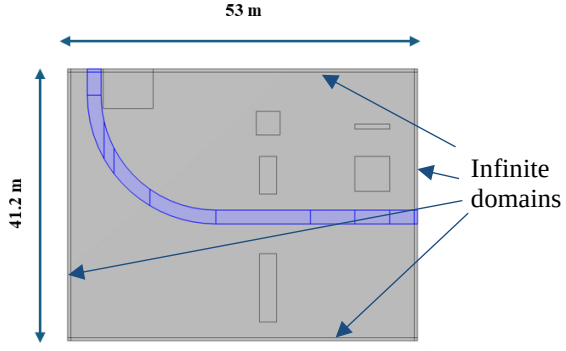

Figure 4. Dimensions (LV trough highlighted).

The material within the troughs, between the troughs and the cables, is air, thus, Surface-to-surface radiation mechanism is taking place. Furthermore, natural convection is considered within the troughs using vertical walls and horizontal plates boundary conditions (Figure 5).

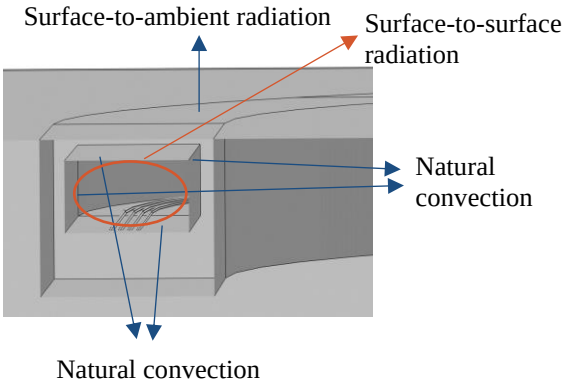

Figure 5. Heat transfer mechanisms in LV trough.

Other cables or parts of cables are installed within ducts (Figure 6).

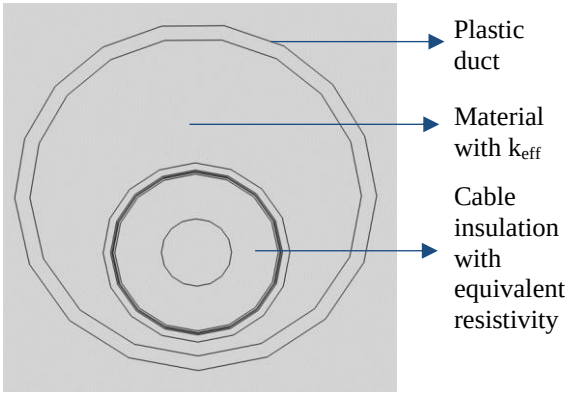

Figure 6. Cable installed inside duct.

To represent the material between the air-filled ducts and the cables, the approach described in IEC 60287-2-1 [1] has been followed, which includes both convective and radiative effects. The duct is filled with air that has an effective thermal conductivity (1):

$$k_{eff} = \frac{1}{\rho_{eff}} \tag{1}$$

where k_{eff} is the effective thermal conductivity, ρ_{eff} is the effective thermal resistivity, which is calculated from thermal resistance T_4' according to [1] (2):

$$\rho_{eff} = \frac{T_4' \cdot 2 \cdot \pi}{\ln(\frac{D_{duct-in}}{D_e})} \tag{2}$$

where $D_{duct-in}$ is the internal diameter of the duct, D_e is the external diameter of the cable and T_4' is the thermal resistance between cable and duct given by the equation (3) [1]:

$$T_4' = \frac{U}{1 + 0.1 \cdot (V + Y \cdot \theta_m) \cdot D_e} \tag{3}$$

where U, V, Y are constants, depending on installation conditions (for cables inside plastic ducts U = 1.87, V = 0.312 and Y = 0.0037) and θ_m is the mean temperature of the medium filling the space between the cable and the duct.

Geometry and meshing optimization

Due to the extremely large size (53 x 41.2 m) and the complexity of the configuration (Figure 4), the geometry is designed using a CAD software and imported to Comsol. As a consequence of the import operation, some layers are not imported properly, and the geometry has to be modified using virtual operations and other techniques. The different domains are, then, sectionalised depending on their installation condition, to be able to build a successful mesh later on.

From Figure 6 above, it can be seen that not all the cable layers are drawn. This technique is used to simplify the geometry and reduce the number of domains by removing domains with very small dimensions and considering a domain with equivalent material properties. It is valid in this case, since we conduct a steady state analysis. For example, the insulation domain includes the inner and outer semiconductive layers by having an equivalent resistivity assigned to it, according to equations (4) and (5):

$$T_{1,eq} = T_{1,1} + T_{1,2} + \cdots + T_{1,n} \tag{4}$$

$$\rho_{eq} = \sum_{i=2}^{n} \rho_{i-1} \cdot \ln(\frac{d_i}{d_{i-1}}) \tag{5}$$

Selections feature becomes critical for so complex geometries. It is apparent that a high number of domains may result to incorrect selections if performed manually, while it would be very time consuming. The boundaries and domains are selected to facilitate the assignment of material properties, the allocation of cable losses and the application of convective and radiative boundary conditions.

Perhaps the biggest challenge for this type of analysis is the mesh creation. The cable layers are represented by cylinders with very small dimensions compared to the rest of the geometry. Moreover, the distance between the cables is very small in some cases, while the cables are bent, which makes swept

mesh of the cable layers questionable. To overcome this, the bent area is split into smaller domains, which can be meshed using the swept method, while the remaining domains are meshed using free tetrahedral elements. To achieve a successful soil mesh of manageable size, the soil domain is split into smaller rectangular domains (fictitious backfills), which can be easily meshed by means of swept operation. The fictitious backfill materials have the same material properties as the soil, since their sole purpose is to simplify the mesh process, as shown in Figure 7.

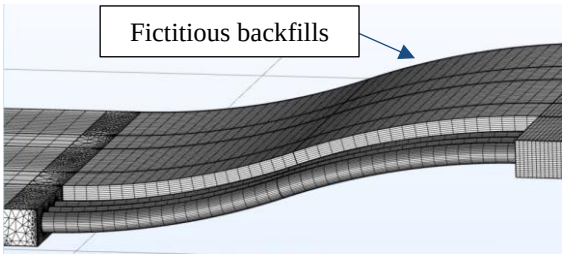

Figure 7. Mesh configuration (swept, free tetrahedral).

The use of swept mesh significantly reduces mesh size and improves solution time, while the accuracy is kept at relatively good levels by increasing the mesh density along the swept mesh. This way, the temperature gradient along conductors, expected due to longitudinal heat cooling, can be well captured.

The mesh and solution time for this model are shown in Table 2.

Table 2. Mesh and solution time.

Operation	Time
Meshing	1 hour
Computing	5.5 hours

Solver configuration

Different solver configurations are examined; Due to the large mesh size (around 21.5 million domain elements) linear discretization (leading to almost 9 million degrees of freedom) with the more consistent direct solver is selected. An extensive sensitivity analysis against mesh is performed and the finest mesh, no longer affecting the derived temperature results, is eventually selected. Additionally, the solver tolerance is reduced at 10^{-6}, to allow for greater accuracy.

Simulation Results

The temperature distribution along the cable installation and the maximum temperature on the conductors are presented in Figure 8. The maximum temperature is observed on the middle phase of the central circuit of the HV cables.

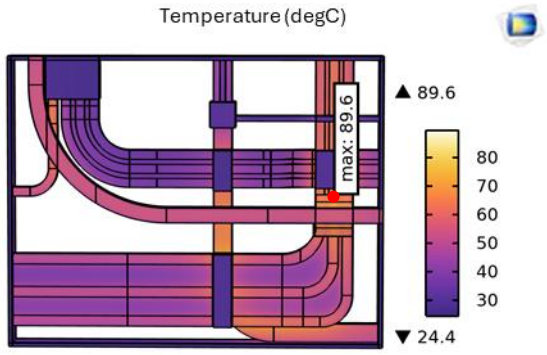

Figure 8. Temperature distribution along cable crossings.

In more detail, the temperature profile along the cables of interest (LV and HV cables 1) is demonstrated in Figure 9 and Figure 10 respectively.

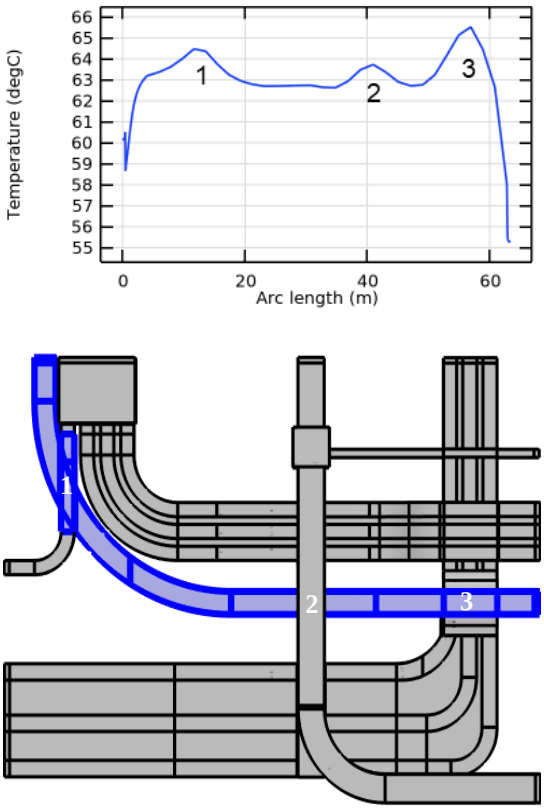

Figure 9. Temperature along LV conductor.

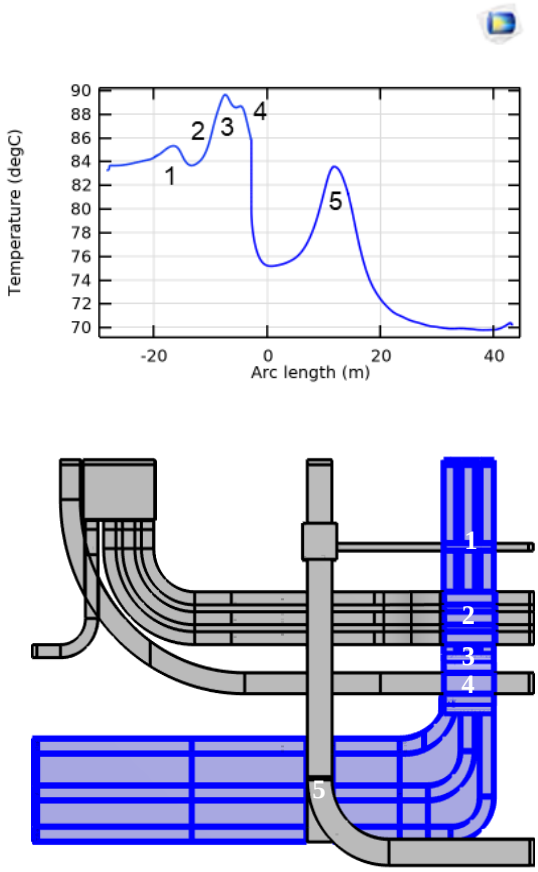

Figure 10. Temperature along hottest phase of HV conductor (HV Cables 1).

In both cases (Figure 9 and Figure 10), the peaks represent the hot spots close to the crossings. In the case of the LV cables, Figure 9 shows the temperature distribution along the length of the cable starting from left to right. The far left and far right temperature values are observed in the infinite domains on the respective side. The value of the temperature in the far-left side is higher than the one observed in the infinite domains on the other side. This is explained due to the fact that the LV cables are in shorter distance with other cables (HV and EHV cables) on the far-left side. At peak number 1, the LV cables are in crossing with the HV cables, while at peak number 2, there is a crossing between the LV cables and the MV and EHV cables. Finally, peak number 3 is observed in the crossing between the LV cables and the HV cables.

The temperature distribution along the HV cables 1 is demonstrated in Figure 10. The highest temperature value is observed at point number 3 (between their crossing with EHV and LV cables). Peaks number 1, 2 and 4 represent the crossing between the HV cables and the MV, EHV and LV respectively. The HV cables 1 after point 2 are buried deeper to avoid collision with the LV trough, while they return to their original depth after their crossing with the LV cables. The temperature values at the infinite domains can be again explained as in the case of the LV cables (Figure 9).

The temperature is also affected by the actual backfill materials (sand, fine sand and concrete), which, have better thermal performance (Table 1) compared to soil.

A graph showing the temperature distribution of the hottest phase of the HV cables produced by the proposed methodology and the method of [8] is shown below (Figure 11):

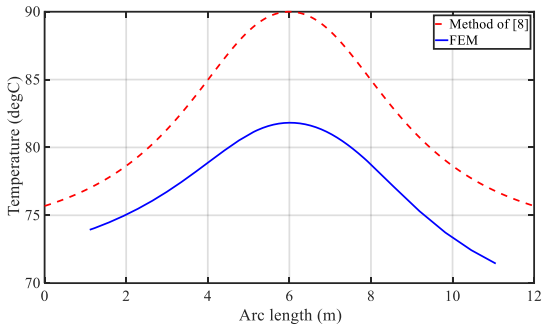

Figure 11. Temperature profile along hottest phase of HV cables 1.

A comparison between the existing method described in [8] and the proposed methodology confirms that the results produced by the proposed methodology are more accurate compared to the previous method and explainable by the installation conditions. This is mainly due to the analytical nature of [8], which inevitably introduces the following limitations:

1. The bending of the cables and the change of installation depth is not considered in the existing method [8], which can only be used for straight crossed cables.
2. Furthermore, it can be observed that the distance between the HV circuits varies along the cable route, and this is another limitation of the method [8], which considers equi-spaced circuits.
3. The existence of multilayer soil (sand, concrete, etc.) and different installation conditions, for example troughs along the route, is not taken into account, since the method [8] accounts for a uniform soil.

Conclusions

The method described in [8] has been already validated with 3D FEM and other commercial software. However, it presents some limitations when it comes to actual installations, such as in High Voltage substations, which include cables installed at different burial depths, bending along their route or installed in multilayer soils.

The proposed methodology presented in this paper, utilizes 3D FEM and it is the only method currently available, which allows to observe the temperature distribution along complex crossings, for example,

when the cables are bent before reaching the crossing point.
One limitation of this model is the extremely high number of mesh elements, leading to a much higher number of degrees of freedom. Another limitation is that any magnetic interaction between the cables has been omitted for simplicity and only the thermal effect of the crossings is considered.

References

[1] *IEC 60287-2-1: Electric cables – Calculation of the current rating – Part 2-1: Thermal resistance - Calculation of thermal resistance,* IEC, 2023.

[2] G. J. Anders, H. Brakelmann, "Cable crossings - Derating considerations - Part I - Derivation of derating equations," *IEEE Trans. Power Del.* , vol. 14, no. 3, pp. 709-714, 1999.

[3] G. J. Anders, H. Brakelmann, "Cable crossings - Derating considerations - Part II - Example of derivation of derating curves," *IEEE Trans. Power Del.*, vol. 14, no. 3, pp. 715-720, 1999.

[4] Anders, G. J., "Rating of electric power cables in unfavorable thermal environment," IEEE Press & Wiley-Interscience, New Jersey, USA, 2005.

[5] E. Dorison, "Cable crossings," in *JICABLE*, 2003.

[6] E. D. G. J. Anders, "Derating factor for cable crossings with consideration of longitudinal heat flow in cable screen," *IEEE Trans. Power Del.*, vol. 19, no. 3, pp. 926-932, 2004.

[7] *IEC 60287-3-3 - Electric cables - Calculation of the current rating - Part 3-3: Sections on operating conditions - Cables crossing external heat sources,* 2007.

[8] A. I. Chrysochos, D. Chatzipetros, D. G. Kontelis, "Ampacity Calculation of Multiple Cables with Different Crossing Angles," in *11th International Conference on Insulated Power Cables*, Lyon, 2023.

[9] *IEC 60287-1-1: Electric cables – Calculation of the current rating – Part 1-1: Current rating equations (100% load factor) and calculation of losses - General,* IEC, 2023.

[10] *CIGRE Technical Brocure 640, "A Guide for Rating Calculations of Insulated Cables", CIGRE,* 2015.

[11] A. I. Chrysochos et al., "Determination of soil thermal resistance: A holistic approach," in *CIGRE*, France, 2022.

[12] A. I. Chrysochos et al., "Rigorous calculation of external thermal resistance in non-uniform soils," in *CIGRE*, France, 2020.